Supporting Information

Enhanced Ultra High Frequency EMI shielding with controlled ITO Nano-Branches Width via Different Tin Material Types

Youngho Kim[a,b,#], Noeul Kim[a,b,#], Sang Hoon Lee[c], Seok-Ki Hyeong[a,d], Jae-Hyun Lee[a], Jaeyeong Lee[e], Jong Seong Bae[e], In Sun Cho[a], Jae-Young Choi[c,f,], Soo Young Kim[b,]*, Hak Ki Yu[a,]**

#: authors equally contributed

[a] Department of Materials Science and Engineering and Department of Energy Systems Research, Ajou University, Suwon 16499, Republic of Korea

[b] Department of Materials Science and Engineering, Korea University, 145 Anam-ro, Seongbuk-gu, Seoul, 02841, Republic of Korea

[c] School of Advanced Materials Science and Engineering, Sungkyunkwan University, Suwon 16419, Republic of Korea

[d] Functional Composite Materials Research Center, Institute of Advanced Composite Materials, Korea Institute of Science and Technology (KIST), 92 Chudong-ro, Bongdong-eup, Wanju-gun, Jeonbuk-do, 55324, Republic of Korea

[e] Korea Basic Science Institute, Busan Center, Busan 46742, Republic of Korea

[f] SKKU Advanced Institute of Nanotechnology (SAINT), Sungkyunkwan University, Suwon 16419, Republic of Korea

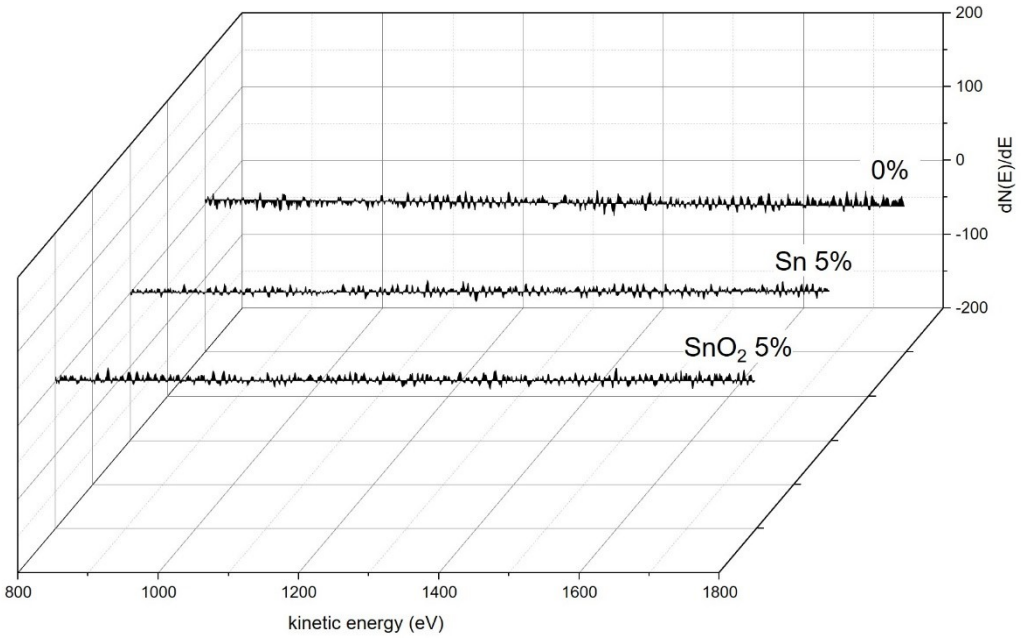

Figure S1. Auger spectroscopy (kinetic energy range: 800–1800 eV) of the initial self-metal dot catalyst for the VLS process according to the Sn precursor (deposited for 3 min).

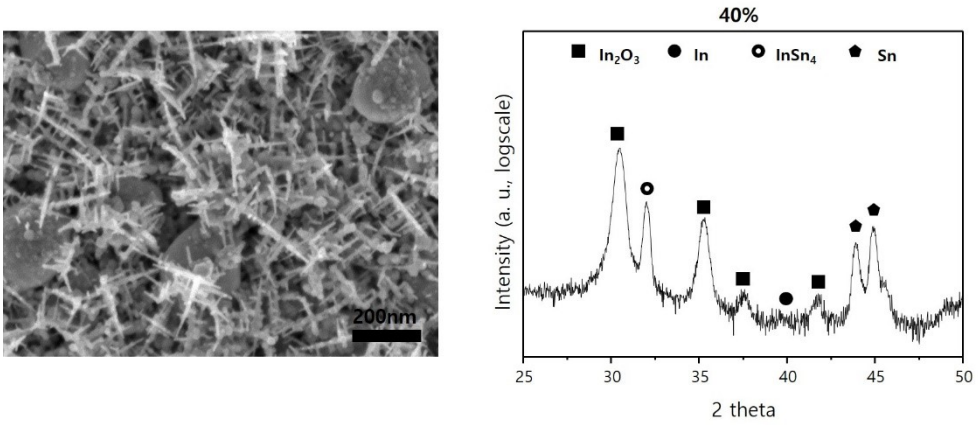

Figure S2. SEM image and XRD pattern of the nanostructure for a SnO_2 concentration of 40%.

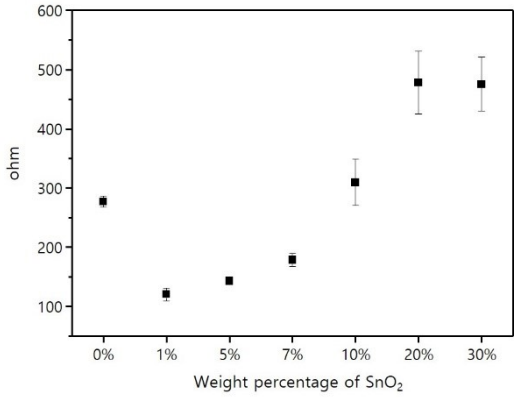

Figure S3. Resistance of the ITO nanostructure according to the SnO_2 concentration (deposited for 20 min).

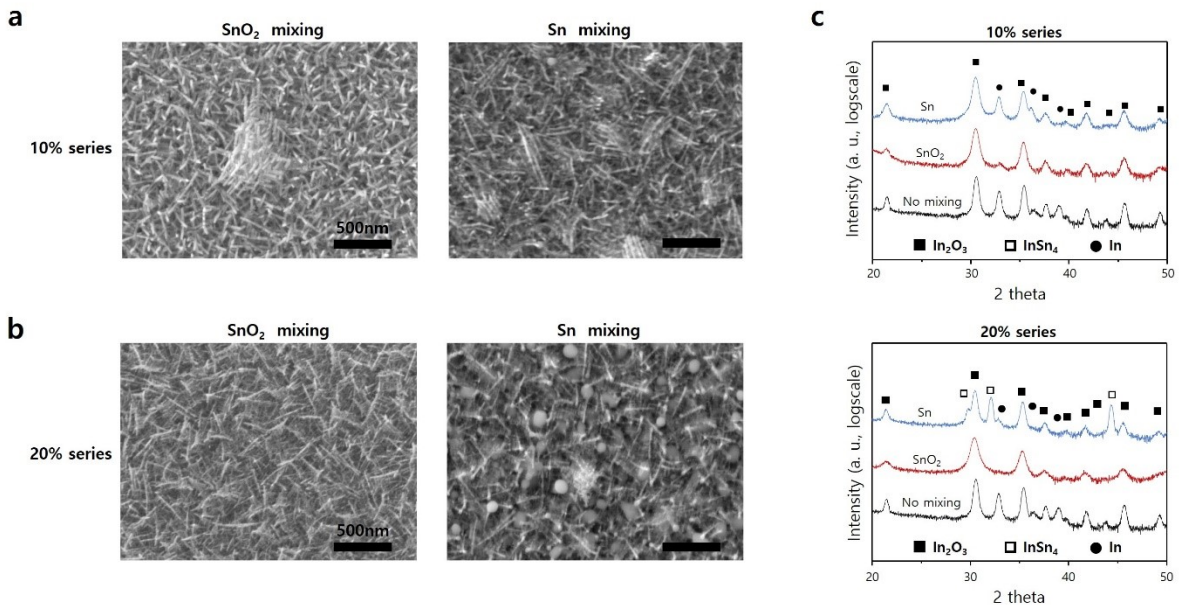

Figure S4. SEM images of the (a) 10% and (b) 20% series according to the Sn precursor. (c) XRD patterns of the 10% and 20% series according to the Sn precursor.

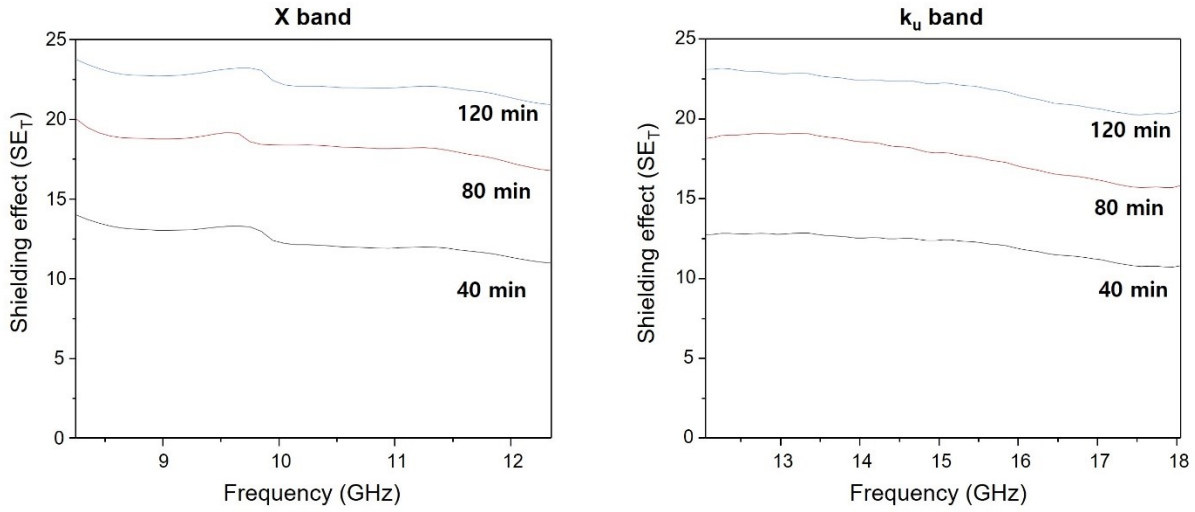

Figure S5. Shielding effects of ITO NBs on a PI film according to the deposition time for the X and K_u bands.

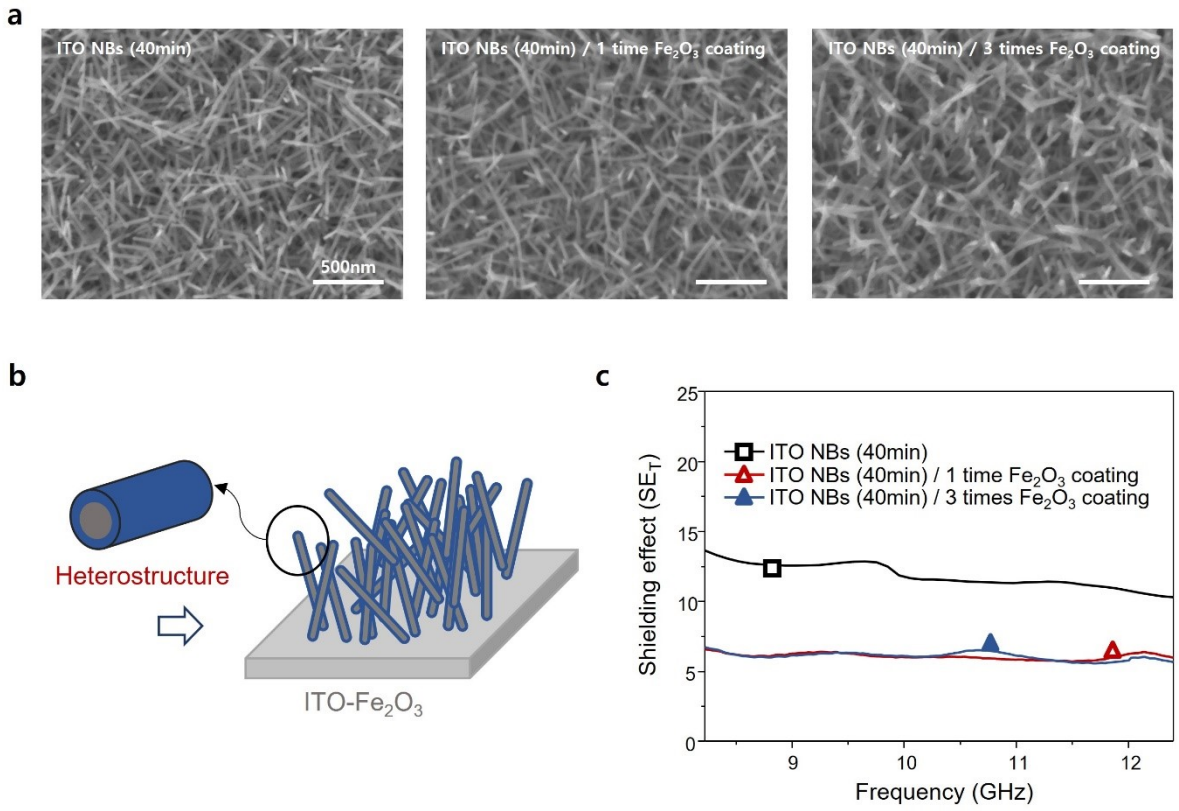

Figure S6. (a) SEM images of bare ITO NBs and ITO NBs with one and three cycles of Fe_2O_3 coating. (b) Schematic of the Fe_2O_3-coated ITO NBs. (c) Shielding effect of the Fe_2O_3-coated ITO NBs in the X band.

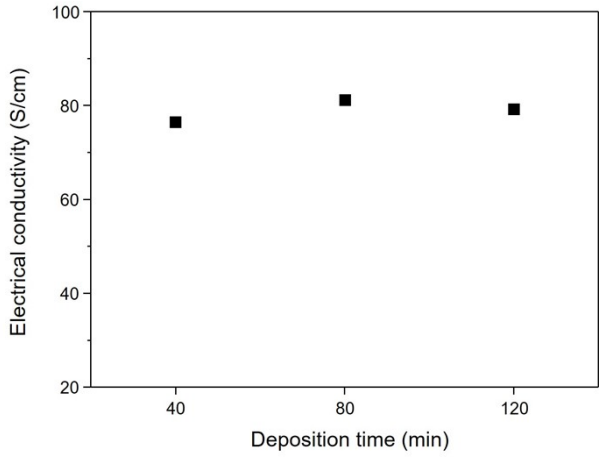

Figure S7. Electrical conductivity of ITO NBs on a PI film according to the deposition time.

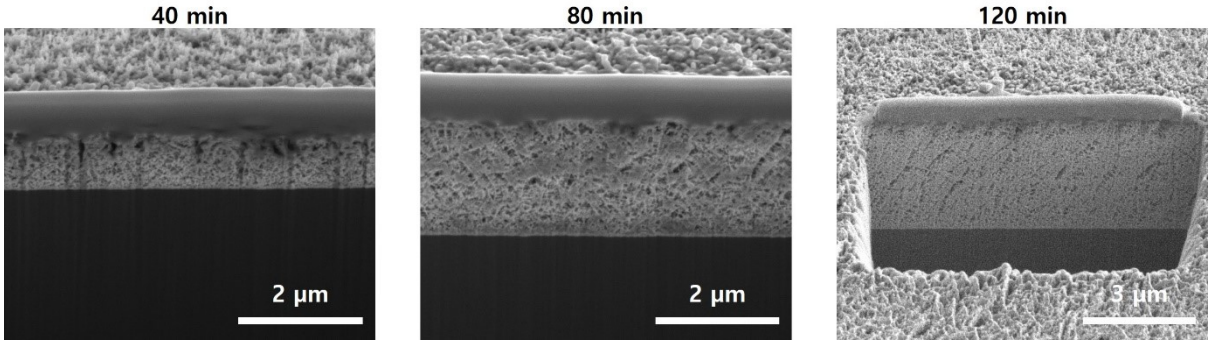

Figure S8. SEM cross-section images of the ITO nanostructures with a SnO_2 concentration of 20% according to the deposition time.

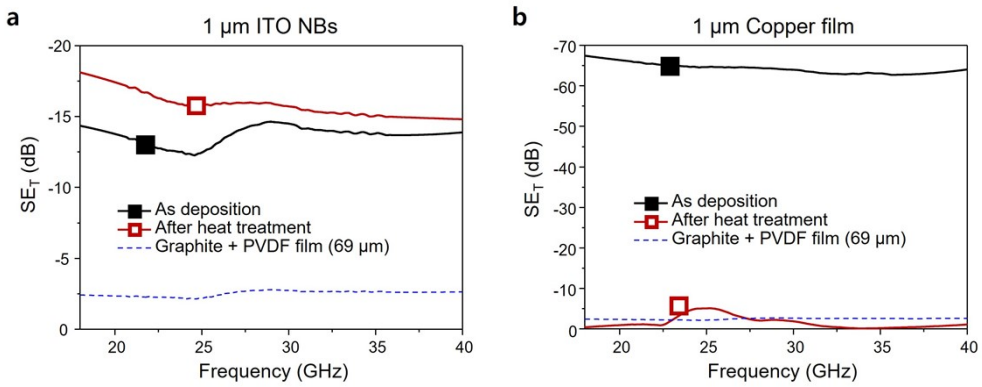

Figure S9. Shielding effects of ITO NBs, copper film, Graphite + PVDF composite